Synthetic nano-scale fibrous extracellular matrix

Peter X. Ma, Ruiyun Zhang
Department of Biologic and Materials Sciences, 1011 North University Avenue, Room 2211, University of Michigan, Ann Arbor, Michigan 48109

Received 26 June 1998; revised 1 December 1998; accepted 15 December 1998

Abstract: Biodegradable polymers have been widely used as scaffolding materials to regenerate new tissues. To mimic natural extracellular matrix architecture, a novel highly porous structure, which is a three-dimensional interconnected fibrous network with a fiber diameter ranging from 50 to 500 nm, has been created from biodegradable aliphatic polyesters in this work. A porosity as high as 98.5% has been achieved. These nano-fibrous matrices were prepared from the polymer solutions by a procedure involving thermally induced gelation, solvent exchange, and freeze-drying. The effects of polymer concentration, thermal annealing, solvent exchange, and freezing temperature before freeze-drying on the nano-scale structures were studied. In general, at a high gelation temperature, a platelet-like structure was formed. At a low gelation temperature, the nano-fibrous structure was formed. Under the conditions for nano-fibrous matrix formation, the average fiber diameter (160–170 nm) did not change statistically with polymer concentration or gelation temperature. The porosity decreased with polymer concentration. The mechanical properties (Young's modulus and tensile strength) increased with polymer concentration. A surface-to-volume ratio of the nano-fibrous matrices was two to three orders of magnitude higher than those of fibrous nonwoven fabrics fabricated with the textile technology or foams fabricated with a particulate-leaching technique. This synthetic analogue of natural extracellular matrix combined the advantages of synthetic biodegradable polymers and the nano-scale architecture of extracellular matrix, and may provide a better environment for cell attachment and function. © 1999 John Wiley & Sons, Inc. J Biomed Mater Res, 46, 60–72, 1999.

Key words: scaffold; tissue engineering; polymer; matrix; fiber; morphology

INTRODUCTION

Much interest has been generated recently in the area of tissue engineering to create biological alternatives for implants and prostheses.[1,2] In this approach, a highly porous scaffold (artificial extracellular matrix) is needed to accommodate cells and guide their growth and tissue regeneration in three dimensions. Biodegradable polymers, either natural[3–5] or synthetic,[6–11] have been processed into scaffolds for tissue engineering.

Collagen is a natural extracellular matrix component of many tissues such as bone, skin, tendon, ligament, and other connective tissues. The fibrillar structure has long been noticed to be important for cell attachment, proliferation, and differentiated function in tissue culture.[12–14] Collagen has also been used for three-dimensional tissue regeneration.[3–5] Collagen fiber bundles vary in diameter from 50 to 500 nm.[12,15] As a natural extracellular matrix component, collagen provides cellular recognition. On the one hand, cellular recognition can be an advantage for regulating cell attachment and function. On the other hand, cellular recognition can be a disadvantage, which is the concern of immunogenecity.[16] There is also less control over the mechanical properties, biodegradability, and batch to batch consistency of natural materials from biological sources.

Aliphatic polyesters such as poly(lactide), poly(glycolide), and their copolymers are biodegradable,[6,10] and biocompatible,[17,18] and among the few synthetic polymers approved by the Food and Drug Administration (FDA) for certain human clinical applications such as surgical sutures and some implantable devices. Therefore, they are widely used as scaffolding polymers. Particulate leaching is a well-documented technique to fabricate porous foams of these polymers for tissue engineering.[7,10,19–21] Textile technologies are used to fabricate biodegradable woven or nonwoven fabrics as tissue engineering scaffolds.[6,9,22] The fibrillar structure of these woven and nonwoven matrices may provide certain advantages. This has been coincided with the fact that various tissues such as cartilage,[9,23] tendon,[24,25] bone,[26] heart valve,[11,27–30] and blood vessel[22,31] have been engineered using these fi-

Correspondence to: P. X. Ma; e-mail: mapx@umich.edu

 CCC 0021-9304/99/010060-13

brous scaffolds. However, the diameter of these fibers is around 15 μm, which is far thicker than that of collagen fibers (50–500 nm). There might be a reason why nature has selected a matrix fiber diameter in the nanometer scale. To mimic the three-dimensional structure of natural collagen matrix and overcome the potential immunogenecity, synthetic fibrillar matrices with a fiber diameter ranging from 50 to 500 nm were created from biodegradable aliphatic polyesters in this work.

EXPERIMENTAL

Materials

Poly(L-lactic acid) (PLLA) and poly(D-L-lactic acid-*co*-glycolic acid) (85/15) (PLGA) with an inherent viscosity of approximately 1.6 and 0.5–0.6, respectively, were purchased from Boehringer Ingelheim (Ingelheim, Germany). Poly(D-L-lactic acid) (PDLLA) with a molecular weight of 103,000 was from Sigma Chemical Co. (St. Louis, MO). PLLA, PLGA, and PDLLA were used without further purification. Tetrahydrofuran (THF), *N,N*-dimethylformamide (DMF), pyridine, dioxane, methanol, and acetone were from Aldrich Chemical (Milwaukee, WI). Deionized water was obtained with a Milli-Q water filter system from Millipore Corporation (Bedford, MA).

Matrix fabrication

The nano-scale fibrous matrices were fabricated typically with five steps: polymer dissolution, phase separation and gelatin, solvent extraction from the gel with water, freezing, and then freeze-drying under vacuum. A typical procedure was used as following: (a) PLLA, PLGA, or PDLLA was weighed accurately into a flask, and then a certain amount of solvent such as THF was added into the flask to make a solution with a desired concentration [from 1% (wt/v) to 15% (wt/v)]. It took typically about 2 h to obtain a homogeneous solution (polymer concentration of 5% or lower) when stirred with a magnetic stirrer at about 60°C. (b) Two milliliters of PLLA solution (prewarmed to 50°C) was added into a Teflon vial. The vial containing PLLA solution was then rapidly transferred into a refrigerator or a freezer set to a chosen temperature to gel. The gelation time depended on temperature, solvent, and the PLLA concentration of the solution. The gel was kept at the gelling temperature for at least 2 h after gelation. (c) The vial containing the gel was immersed into distilled water for solvent exchange. The water was changed three times a day for 2 days. (d) The gel was removed from water, blotted with a piece of filter paper, and then transferred into a freezer at −18°C for at least 2 h. (e) The frozen gel was transferred into a freeze-drying vessel at −5°~−10°C in an ice/salt bath, and was freeze-dried under vacuum lower than 0.5 mm Hg for 1 week. The dried porous matrix was then stored in a desiccator until characterization.

Characterization

The gelation time was determined as the time period from the time point when the sample was set to the gelling temperature to that when the the sample (held at this temperature) could no longer flow.

The melting behavior of the fibrous matrices was characterized with a differential scanning calorimeter (DSC-7; Perkin-Elmer, Norwalk, CT). The calibration was performed using indium standards. The fibrous matrix samples (5–10 mg) were used without further thermal treatment. A heating rate of 20°C/min and a temperature range of 30°–200°C were used. The degree of crystallinity was calculated as $X_c = \Delta H_m/\Delta H_m^o$, where ΔH_m was the measured enthalpy of melting and ΔH_m^o was the enthalpy of melting of 100% crystalline polymer. For PLLA, ΔH_m^o = 203.4 J/g.[32]

The estimated densities and porosities of the fibrous matrices were obtained as follows. The circular discs of the fibrous matrices were fabricated as described in the previous section. The diameter and height of a disc was measured to calculate the volume. The weight of the specimen was measured with an analytical balance accurate to 10^{-4} g. The density was calculated from the volume and weight. The porosity, ε, was calculated from the measured overall densities D_f of the fibrous matrix and the skeletal density D_p:

$$\varepsilon = \frac{D_p - D_f}{D_p} \tag{1}$$

For the fibrous matrix, the skeletal density was the density of the polymer, which was given by:

$$D_p = \frac{1}{\dfrac{1 - X_c}{D_a} + \dfrac{X_c}{D_c}} \tag{2}$$

where X_c was the degree of crystallinity of the polymer. For PLLA, D_a = 1.248 g/mL (density of amorphous polymer) and D_c = 1.290 g/mL (density of 100% crystalline polymer).[33]

The morphologies of the fibrous matrices were studied with scanning electron microscopy (SEM) (S-3200N; Hitachi, Japan) at 15 kV. The specimens were cut with a razor blade or fractured after being frozen in liquid nitrogen for 5 min, and were then coated with gold using a sputter coater (Desk-II; Denton Vacuum Inc.). The gas pressure was lower than 50 mtorr, and the current was about 40 mA. The coating time was 200 s.

The average fiber diameter was calculated from the SEM micrographs. Eighty fibers were measured for each sample. Their averages and standard deviations were reported. The surface-area-to-volume ratio was estimated based on the average fiber diameter. The surface areas of the fiber ends were neglected based on a very large aspect ratio of the fibers (virtually a continuous fiber network), so that the surface area of a fiber was calculated with the equation

$$A_f = \pi \cdot d \cdot l \tag{3}$$

where d was the diameter of the fiber and l was the length of the fiber. The volume of a fiber was given by

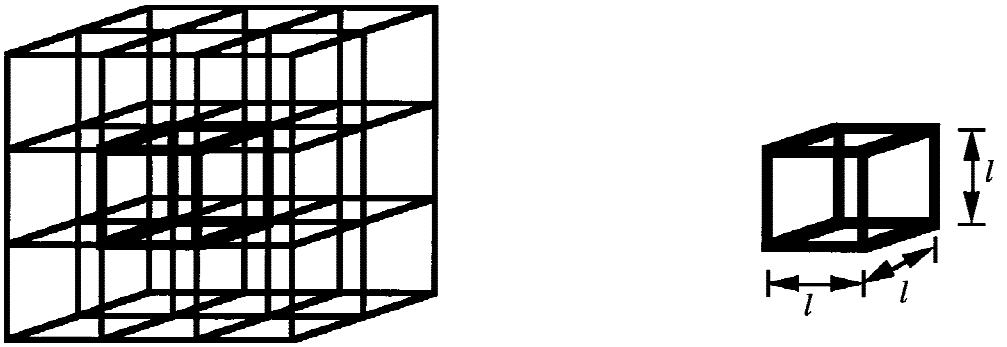

Figure 1. The cubic fiber network model.

$$V_f = \frac{\pi \cdot d^2 \cdot l}{4} \tag{4}$$

Therefore, the surface-to-volume ratio was given by

$$\frac{A_f}{V_f} = \frac{\pi \cdot d \cdot l}{\frac{\pi \cdot d^2 \cdot l}{4}} = \frac{4}{d} \tag{5}$$

To quantify the fiber network density, the fiber length between two conjunctions (unit length) was estimated based on a simplified cubic stucture model (Fig. 1). There were 12 unit fibers bordering each unit cube. Four unit cubes shared each of these fibers. Therefore, there were three unit fibers in each unit cube. The porosity of the fiber network was given by

$$\varepsilon = 1 - \frac{3V_f}{V_c} \tag{6}$$

where V_f was the volume of one unit fiber and V_c was the volume of the unit cube. Substituting Equation (4) and $V_c = l^3$ into Equation (6), the porosity was given by

$$\varepsilon = 1 - \frac{\frac{3\pi \cdot d^2 \cdot l}{4}}{l^3} \tag{7}$$

The unit length was given by rearranging Equation (7),

$$l = \frac{d}{2}\sqrt{\frac{3\pi}{1-\varepsilon}} \tag{8}$$

When the fiber diameters were compared, a two-tail Student t test (assuming equal variances) was performed to determine the statistical significance ($p < .05$).

Uniaxial tensile mechanical testing was performed to measure the mechanical properties of the nano-scale fibrous matrices using methods similar to those for the mechanical testing of natural and engineered tendon, heart valve, and their scaffolding matrices,[11,25,27] with an Instron 4502 mechanical tester (Instron Corporation, Canton, MA). The matrix sheets with dimensions of 90 × 60 × 3 mm^3 were prepared, and then cut into 90 × 10 × 3-mm^3 strips for mechanical testing. A gauge length of 40 mm (distance between two grips) and a crosshead speed of 5 mm/min were used. Six specimens were tested for each sample. The averages and standard deviations from the specimens fractured in the middle (four to six) are reported.

RESULTS

A series of highly porous (up to 98.5% porosity) nano-scale fibrillar matrices was created from biodegradable aliphatic polyesters (Table I). The novel porous structure was a three-dimensional continuous fibrous network (Fig. 2), which was similar to a natural collagen matrix. The diameter of the fibers ranged from 50 to 500 nm, which was also the same diameter range of natural collagen fibers.

To create this unique fibrillar matrix structure, gelation was a critical step. The gelation behavior of PLLA in various solvents was studied to understand

TABLE I
Density and Porosity Values of Porous Aliphatic Polyester Matrices

Gelling Temperature (Polymer Concentration)	−18°C		8°C		23°C	
	Density (g/mL)	Porosity (%)	Density (g/mL)	Porosity (%)	Density (g/mL)	Porosity (%)
PLLA/THF 1.0%	0.0183	98.5	0.0186	98.5	N/A	N/A
PLLA/THF 2.5%	0.0393	96.9	0.0328	97.4	N/A	N/A
PLLA/THF 5.0%	0.0638	94.9	0.0587	95.3	0.0583	95.4
PLLA/THF 7.5%	0.0889	92.9	0.0885	93.8	0.0781	93.8
PDLLA/(D/W) 5.0%*	0.1996	84.0				
PLGA (D/W) 10%†	0.2359	81.1				

*PDLLA, dioxane/H_2O = 85/15.
†PLGA(85/15), dioxane/H_2O = 80/20.

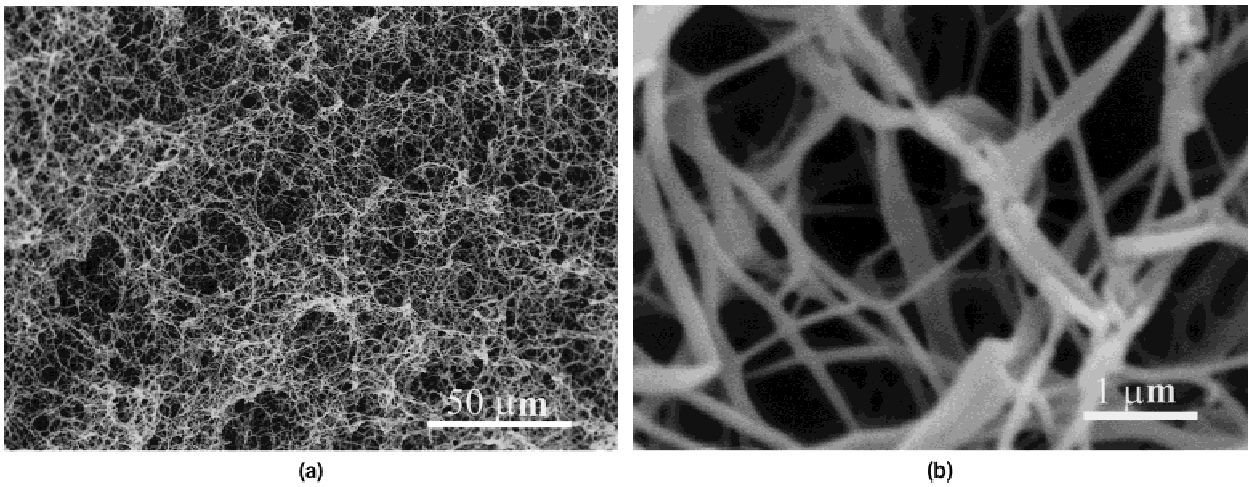

Figure 2. SEM micrographs of a PLLA fibrous matrix prepared from 2.5% (wt/v) PLLA/THF solution at a gelation temperature of 8°C: (a) ×500; (b) ×20K.

the relationship between the gelation and the morphologies of the resultant polymer matrices. Gelation occurred in several solvents and solvent mixtures such as THF, DMF, pyridine, THF/methanol, THF/acetone, dioxane/methanol, dioxane/H_2O, and dioxane/acetone. The gelation time varied with polymer concentration and gelation temperature (Table II). At a temperature of 15°C or lower, gelation occurred readily in a short period of time for all of the PLLA/THF solutions in the concentration range studied. In a different solvent system, THF/methanol (80/20), the nano-fiber structure could only be obtained by quenching the PLLA solution in liquid nitrogen (Fig. 3). The translucent gels prepared from PLLA/THF solution (clear at low PLLA concentrations) became stronger and cloudier over time when stored at the gelation temperature. At temperatures higher than room temperature, gelation occurred only from the solution with a PLLA concentration higher than 3.0% (wt/v), and the gelation took much longer time than that at lower temperatures. In the high-temperature range (19°C or higher), the clear solution had become cloudy with a large amount of small gel particles formed before the whole solution gelled. The turbidity of the gel was higher than those of the gels formed at lower temperatures. For the solutions with a PLLA concentration of 2.5% or lower, small gel particles were formed and suspended in the solution without uniform gel formation after being stored at room temperature for more than 7 days.

The average fiber diameter of the fibrillar matrices did not change statistically with the concentration of polymer solution used to fabricate the matrices in the concentration range studied (Figs. 4 and 5). The average unit length (fiber length between two conjunctions) decreased with increasing polymer concentration (Table III). At very low polymer concentrations such as 1% PLLA/THF solution, relative large pores were obtained with nonuniform interfiber spacing [Fig. 4(a)]. With increasing polymer concentration, the pore structure became increasingly uniform, and the average unit length decreased (Table III). These morphological observations were consistent with the porosity and density data (Table I).

Gelling temperature was another important factor controlling the porous morphology of the matrices

TABLE II
Gelation Behavior of PLLA/THF Solution

Gelation Temperature (°C)	Gelation Time			
	PLLA/THF 1.0% (wt/v)	PLLA/THF 2.5%(wt/v)	PLLA/THF 3.0% (wt/v)	PLLA/THF 5.0% (wt/v)
−18	15 min	12 min	10 min	8 min
8	150 min	40 min	30 min	25 min
15	24 h	6	4 h	50 min
23	MG	MG	12 h	4 h
30	CS	MG	24 h	12 h
35	CS	CS	MG	20 h
40	CS	CS	CS	MG
45	CS	CS	CS	CS

MG-microgel particles were formed and suspended in the solution (cloudy); CS-solution was still clear after 24 h.

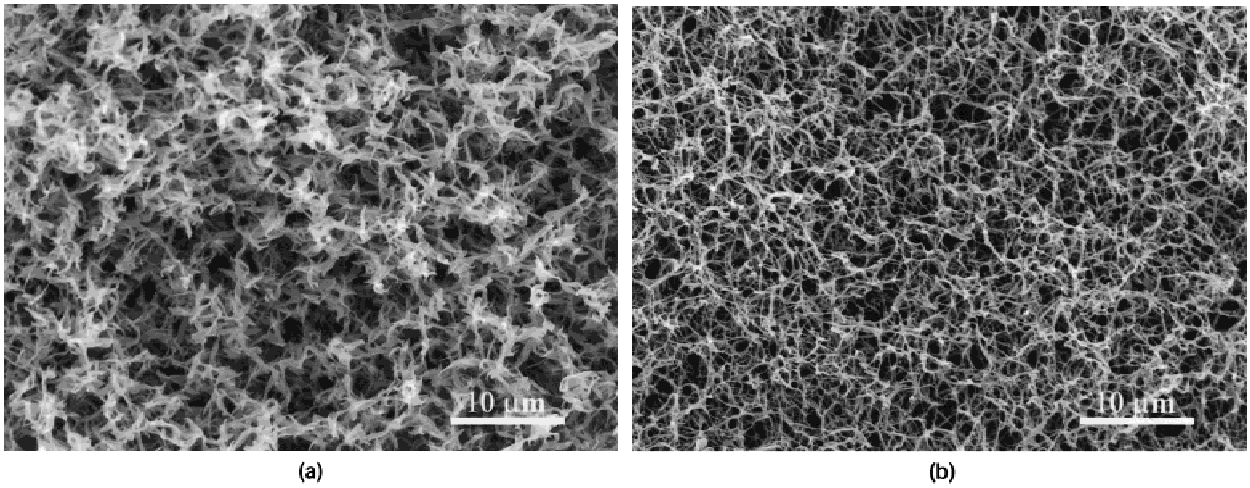

Figure 3. SEM micrographs of PLLA fibrous matrices prepared from 5.0% (wt/v) PLLA/THF/methanol (THF/methanol = 80/20) solution at different gelation temperatures: (a) −18°C, ×2.0K; (b) in liquid nitrogen, ×2.0K.

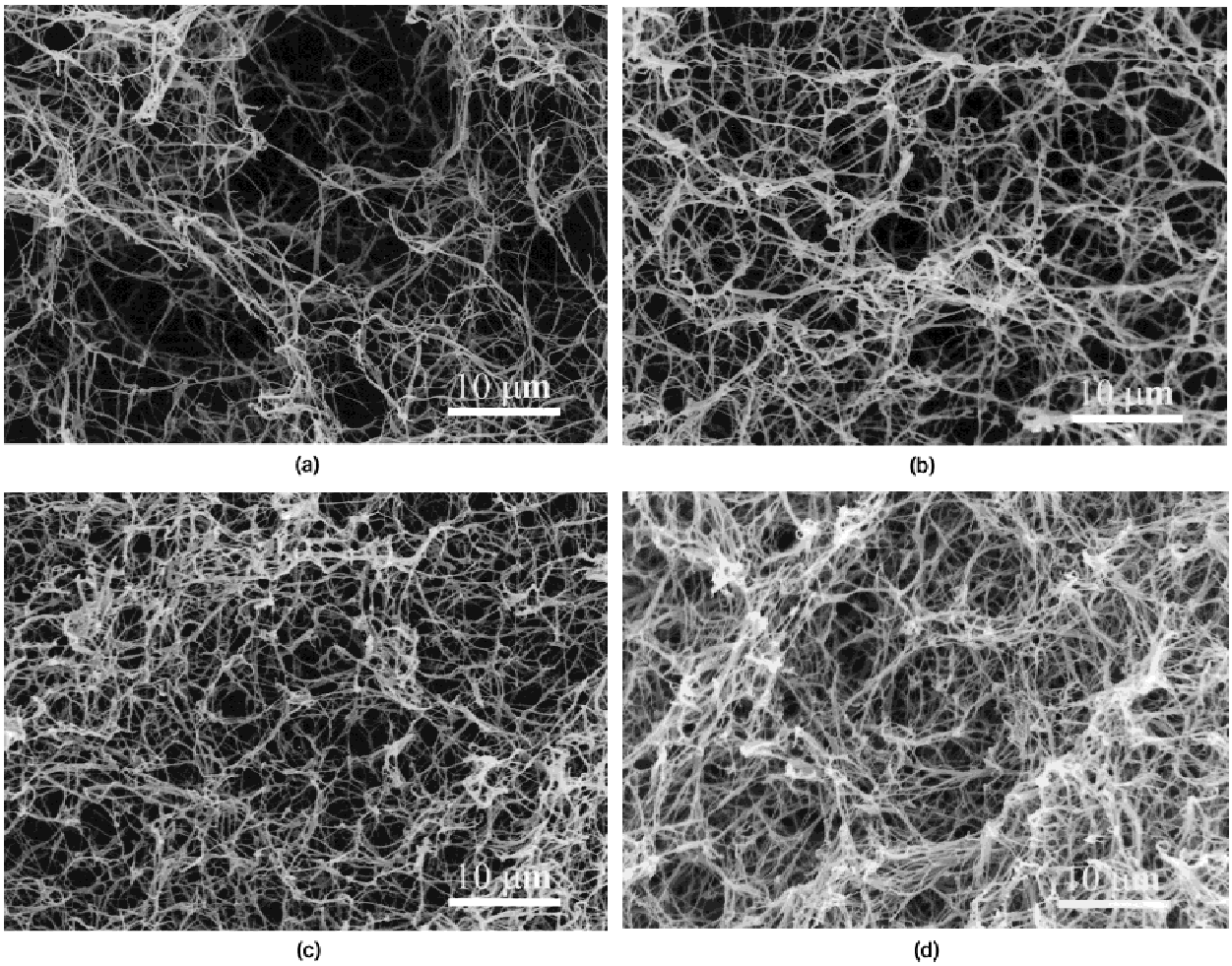

Figure 4. SEM micrographs of PLLA fibrous matrices prepared from PLLA/THF solution with different PLLA concentrations at a gelation temperature of 8°C: (a) 1.0% (wt/v), ×2.0K; (b) 2.5% (wt/v), ×2.0K; (c) 5.0% (wt/v), ×2.0K; (d) 7.5% (wt/v), ×2.0K.

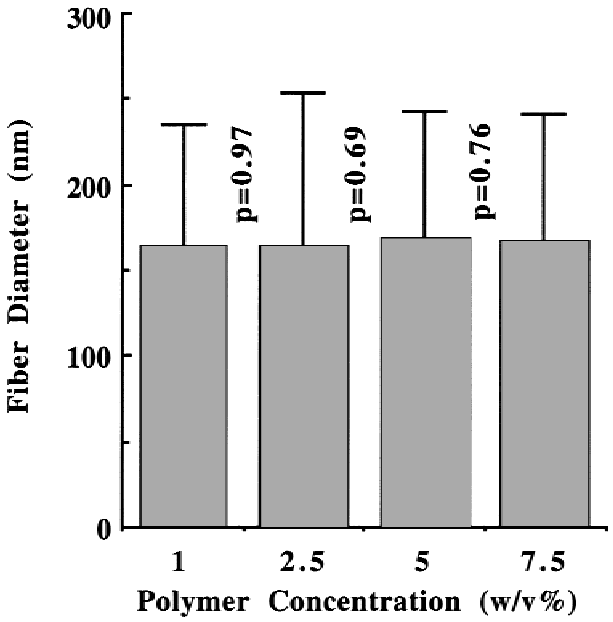

Figure 5. Fiber diameter of PLLA matrix (gelation temperature: 8°C) versus polymer concentration (p values obtained from two-tailed Student t test are listed for comparison between fiber diameters of PLLA matrices).

(Fig. 6). The matrix structure formed via gelation of 5% PLLA/THF solution at 23°C (room temperature) or 19°C was evidently different from that formed at lower gelation temperatures. Platelet-like structure was the only or primary structure [Fig. 6(a,b)]. The size of the platelets was at the micrometer level. Others also obtained similar platelet morphology of foam prepared at room temperature from PLLA solution in acetone.[34] At a gelation temperature of 17°C, both fibrous and plateletlike structures were observed [Fig. 6(c)]. For the matrices formed at lower gelation temperatures such as 15°C, 8°C, and −18°C, or in liquid nitrogen, a three-dimensional nano-fiber network was formed [Fig. 6(c–f)]. The fiber diameter of the matrix did not change with the gelling temperature as long as it was in the fiber-forming temperature range (Fig. 7), while the interfiber spacing became more uniform at lower gelling temperatures [Fig. 6(d–f)].

The melting point, enthalpy of melting, and degree of crystallinity of the matrices prepared from PLLA/THF solution with different PLLA concentrations and at different gelling temperatures were measured with DSC (Table IV). At a gelation temperature of −18°C, the melting point and degree of crystallinity of PLLA matrices did not change significantly with the polymer concentration. The degree of crystallinity did not change significantly with gelation temperature, either, in the lower temperature range (15°C or below). However, the matrix formed at a higher temperature (e.g., room temperature) had a higher degree of crystallinity than those formed at low gelation temperatures (Table IV). PLLA films were also cast from PLLA/THF solution at room temperature. The crystallinity of the cast film was very close to that of the plateletlike matrix formed at room temperature (Table IV). The higher crystallinity of these two PLLA samples (foam and film) could be attributed to the easy rearrangement of PLLA chains in the solution during crystallization at room temperature (crystal nucleation and growth).

TABLE III
Structural Parameters of Nano-Fibrous Matrices Prepared from PLLA/THF Solution of Various Concentrations at Gelation Temperature of −18°C

Concentration (%)	Diameter (nm)	Porosity (%)	Unit Length (nm)	Surface/Volume Ratio (μm^{-1})
1.0	164 ± 71	98.5	2055	24.4
2.5	164 ± 90	97.4	1561	24.4
5.0	169 ± 74	95.3	1197	23.7
7.5	166 ± 74	93.8	1023	24.1

The gelation procedure also had effects on the matrix structure formation. Both plateletlike and nanofiber–like structures were observed for a matrix prepared by annealing a 5% PLLA/THF solution at room temperature for 2 or 12 h and then gelling at −18°C [Fig. 8(a,b)]. The percentage of plateletlike structure increased with the time annealed at room temperature. After 24 h of room temperature annealing, the platelike structure became the only structure observed with or without quenching to −18°C [Fig. 8(c)]. In contrast, when the solution was quenched to −18°C for 10 min at first and then annealed at room temperature for 1 week, the only structure observed was the nano-fiber network [Fig. 8(d)].

Highly porous matrices were also fabricated from PDLLA/THF and PLGA/THF solutions in the same polymer concentration and temperature ranges as those of PLLA/THF solutions. The microstructures of the PDLLA and PLGA matrices were evidently different from those of PLLA matrices prepared with the same procedure (Fig. 9). There was neither a fibrous nor a platelet structure formed from these amorphous polymers. Others also observed a somewhat similar morphology for amorphous polymer foams with a lower porosity prepared for controlled release purpose.[35] No typical gelation was observed for these uncrystallizable polymers in the polymer concentration and gelation temperature ranges studied. This indicated that the crystallization of the polymer might play an important role in the formation of PLLA/THF gels. Small PLLA crystallites formed from PLLA solution might provide physical crosslinks to form the three-dimensional polymer network.

In the water extraction process, a small shrinkage (<5%) of the gels was observed. However, there was no evident difference in the matrix structure prepared from PLLA/dioxane/methanol (80/20) with or without water extraction process (Fig. 10).

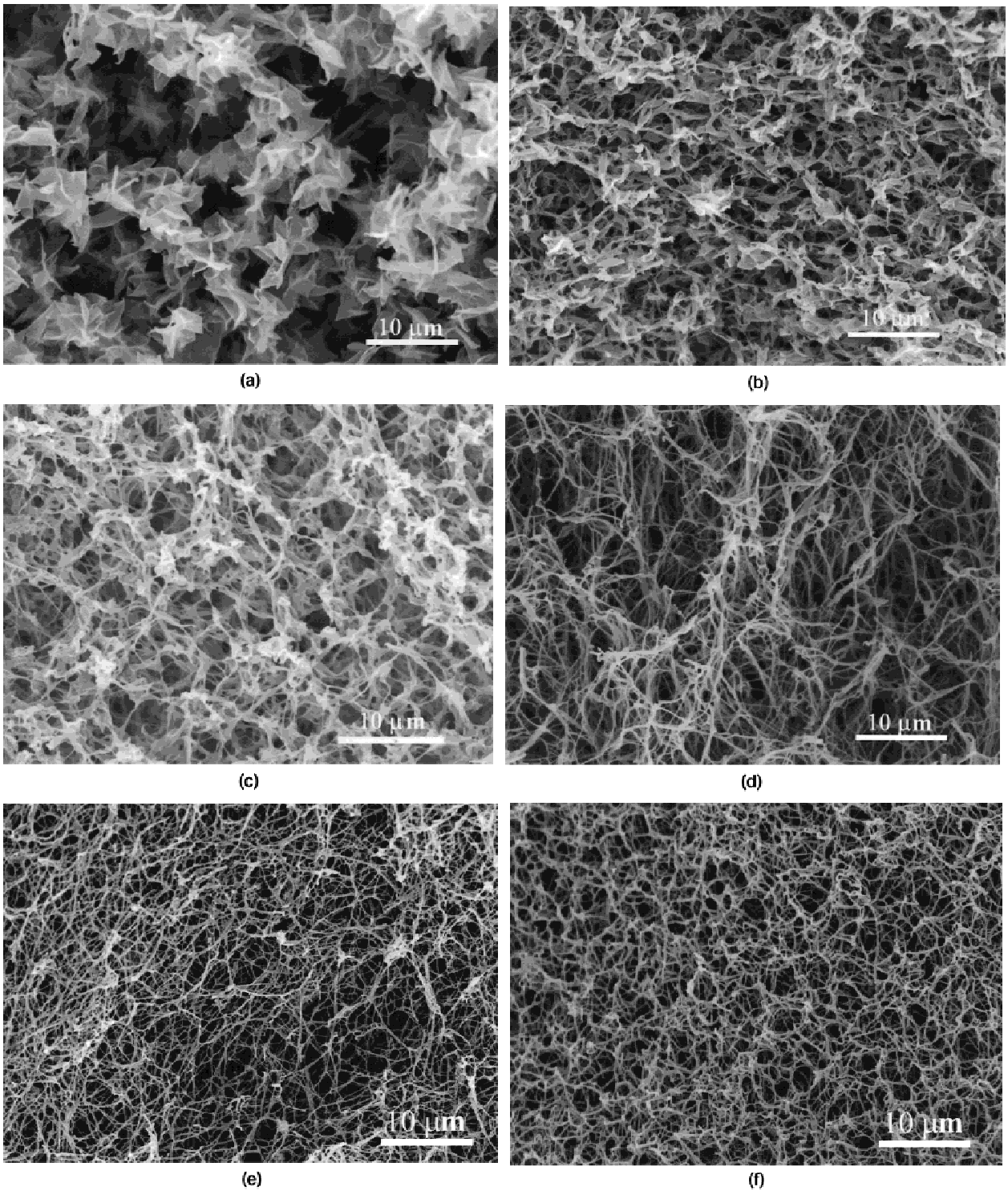

Figure 6. SEM micrographs of PLLA matrices prepared from 5.0% (wt/v) PLLA/THF solution at different gelation temperatures: (a) 23°C, ×2.0K; (b) 19°C, ×2.0K; (c) 17°C, ×2.0K; (d) 15°C, ×2.0K; (e) −18°C, ×2.0K; (f) liquid nitrogen, ×2.0K.

Scanning electron microscopic observation showed that the frozen temperature prior to freeze-drying also affected the morphology of the matrix prepared from a PLLA/THF gel (Fig. 11). The uniform nano-fiber network was formed from the gel frozen in liquid nitrogen. A less uniform matrix structure was formed from the gel frozen at −5°C, presumably owing to large ice crystal formation at the higher frozen temperature, which led to large pore formation after the sublimation of the ice crystals.

The surface/volume ratio (the ratio of surface area to polymer skeleton volume) of the nano-fibrous ma-

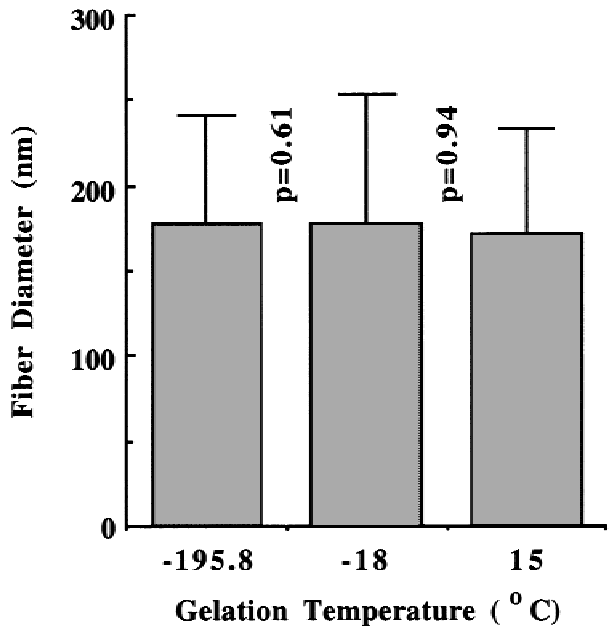

Figure 7. Fiber diameter of PLLA matrix [prepared from 5.0% (wt/v) PLLA/THF solution] versus gelation temperature (p values obtained from two-tailed Student t test are listed for comparison between fiber diameters of PLLA matrices).

trix (~24 μm^{-1}) did not change with the polymer concentration, because the fiber diameter (160–170 nm) did not change with polymer concentration (Table III). The surface/volume ratio of this nano-fibrous matrices was two to three orders of magnitude higher than those of foams prepared with salt-leaching techniques[7] or nonwoven fabrics prepared with the textile technology.[6]

Tensile testing was conducted to measure the mechanical properties of the nano-fibrous matrices (Fig. 12). Young's modulus, tensile strength, and elongation at break all increased with polymer concentration. Mechanical properties of the plateletlike matrices were too weak to measure.

DISCUSSION

One of the most important questions in polymer scaffolding is the cell–polymer interaction. There has been very active research on the effects of surface chemistry on cell–materials interactions. It has been demonstrated that certain bioactive peptides such as RGD-modified surfaces of polymers[36,37] or other materials[38,39] can mimic natural proteins in enhancing cell adhesion in serum-free cell culture medium. There has also been active research on creating porous structures from synthetic polymers to serve as scaffolding for cell attachment, growth, and tissue regeneration in three dimensions.[6,7,10] Textile technologies have been used to fabricate nonwoven fabrics with fiber diameters at the micrometer scale (usually between 10 and 20 μm).[6,9] Particulate-leaching technique is well documented for the fabrication of porous biodegradable polymer foams.[7,10] In this technique, the polymer solution is usually mixed with salt particles (or other water-soluble particles) and cast in a mold. After the evaporation of the solvent, a solid polymer–salt composite is formed. The salt is then leached out with water to generate pores. The pore size and shape are controlled by the salt particles. Thermally induced phase separation techniques have also been widely reported to produce porous foams of biodegradable polymers.[34,35,40–47] These porous foams are fabricated as controlled-release vehicles, implant materials, scaffolding matrices for tissue engineering, or applications in combinations of the above. Because of the complexity of the processing variables involved in phase separation techniques (type of polymer, type of solvent, polymer concentration, phase separation temperature, solvent exchange in some cases, thermal treatment, other procedures involved, and their order), various matrix morphologies have been reported. However, these matrices are different from natural extracellular matrix in architecture. A variety of biodegradable polymers, solvent and solvent mixtures, gelation temperatures, solvent exchanges, heat treatments, and procedure variations have been investigated in this work. Biodegradable polymers are successfully fabricated into nano-fiber matrices to mimic the architecture of a natural extracellular matrix.

These synthetic analogues of natural extracellular matrices combine the advantages of synthetic biodegradable polymers and the architecture of natural ex-

TABLE IV
Melting Behavior and Degree of Crystallinity (X_c) of Porous PLLA Matrices and Cast Film Prepared from PLLA/THF Solution

PLLA/THF Concentration	Gelling Temperature (°C)	T_m (°C)	ΔH_m (J/g)	X_c
1.0% (wt/v)	−18	180.5	49.5	24.4
2.5% (wt/v)	−18	181.6	55.3	27.2
5.0% (wt/v)	−18	179.1	56.0	27.5
7.5% (wt/v)	−18	177.0	53.3	26.2
5.0% (wt/v)	Liquid nitrogen	180.7	56.8	27.9
5.0% (wt/v)	8	183.4	53.2	26.2
5.0% (wt/v)	15	180.2	57.6	28.3
5.0% (wt/v)	23	182.5	74.2	36.5
PLLA film	23	179.3	68.2	33.5

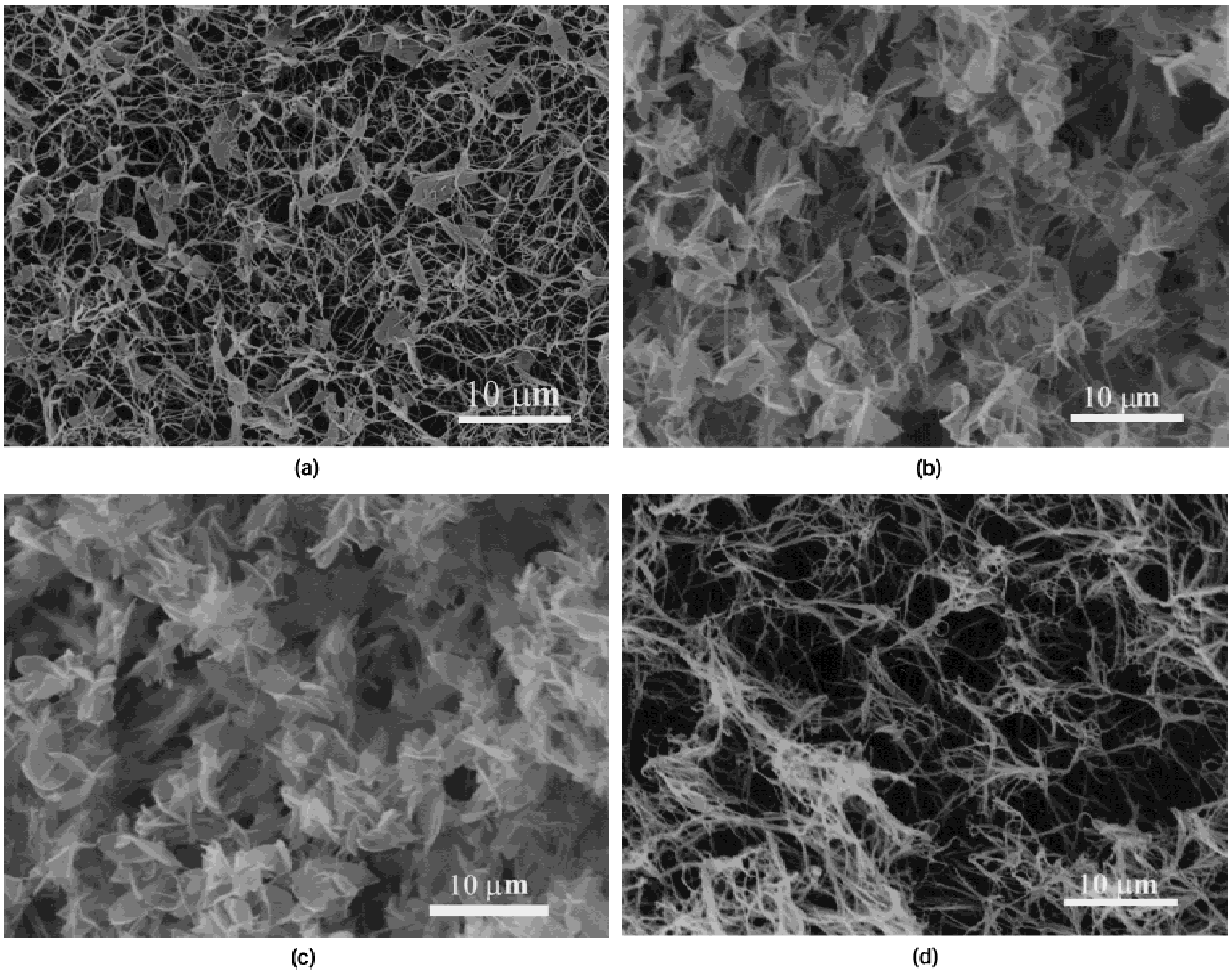

Figure 8. SEM micrographs of PLLA matrices prepared from 5.0% (wt/v) PLLA/THF solution with different thermal gelation history: (a) annealed at room temperature for 2 h, then quenched to −18°C; (b) annealed at room temperature for 12 h, then quenched to −18°C; (c) annealed at room temperature for 24 h, then quenched to −18°C; (d) quenched to −18°C for 10 min, then annealed at room temperature for 1 week.

tracellular matrices, which is speculated to play an important role in cell attachment, migration, growth, and function.[14] In addition to getting away from the immunogenicity concerns, synthetic polymers provide the advantage of controllable degradation (hydrolysis) rate, hydrophilicity, and mechanical properties to fit specific applications. In this work, we have shown how to fabricate biodegradable polymers into nano-fibrillar and various other porous matrices. Their processing, structure, and property relationships are studied.

It is worth noticing that the fibrillar structure was obtained when PLLA/THF solution was quenched in liquid nitrogen [Fig. 6(d)]. Previously, we have shown that when a polymer solution (with several different solvent systems) is cooled fast enough and to a temperature low enough to freeze the solvent into solid state so that there is not enough time for liquid–liquid phase separation to occur, a solid–liquid phase separation will take place.[40] The morphology of the foam formed from a solid–liquid phase separation (solvent crystallization) is very different from the nano-fibrous network. Channels and ladderlike partitions are characteristic features of solid–liquid phase separation.[40,41] These structural features have not been observed in the PLLA/THF system, probably owing to the different phase separation process which occurs before it reaches the freezing temperature of the solvent.

It has also been found that the PLLA matrices formed at a higher gelation temperature (such as room temperature) has a higher crystallinity than that of matrices formed at lower gelation temperatures (15°C or lower). The difference in degree of crystallinity is coincident with the difference in matrix structure. This seems to suggest that at a higher gelation temperature, phase separation occurs through a mechanism different from that at a lower gelation temperature. We hypothesize that the phase separation at higher temperatures (19°C or higher) is due to a crystal nucleation and growth process. The fact that the matrix formed at

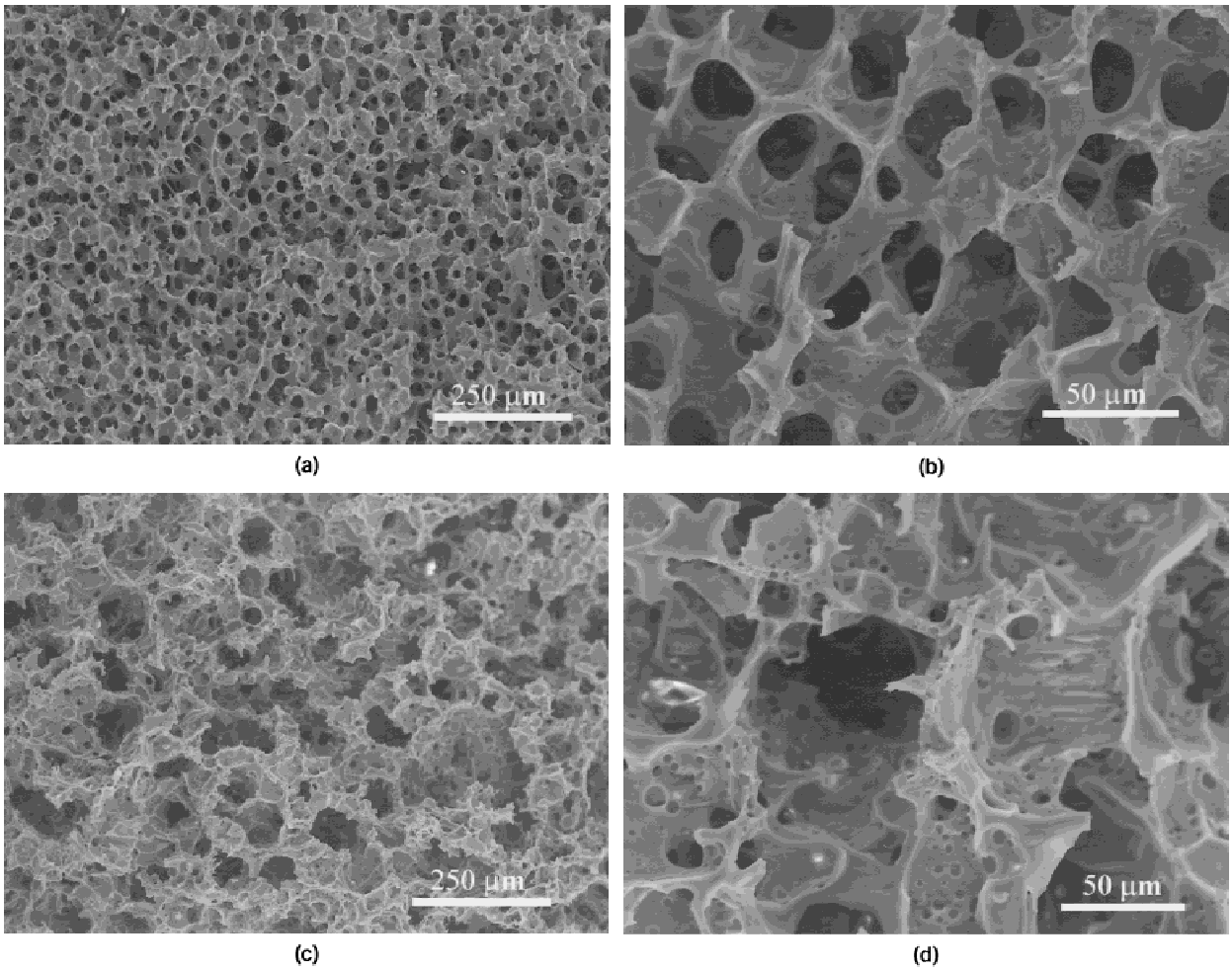

Figure 9. SEM micrographs of porous matrices prepared from uncrystallizable aliphatic polyester solutions at a gelation temperature of −18°C: (a,b) 10% PLGA (85/15)/dioxane/H_2O (dioxane/H_2O = 80/20); (c,d) 5% PDLLA/dioxane/H_2O (dioxane/H_2O = 85/15).

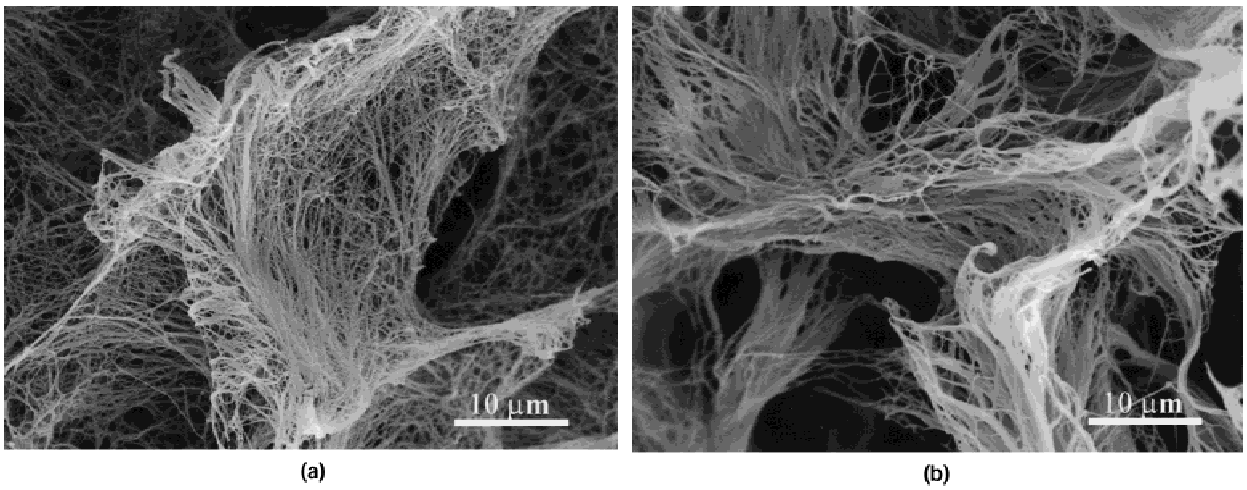

Figure 10. SEM micrographs of PLLA matrices prepared from 2.5% (wt/v) PLLA/dioxane/methanol (dioxane/methanol = 80/20) solution with a gelation temperature of −18°C: (a) with water extraction, ×2.0K; (b) without water extraction, ×2.0K.

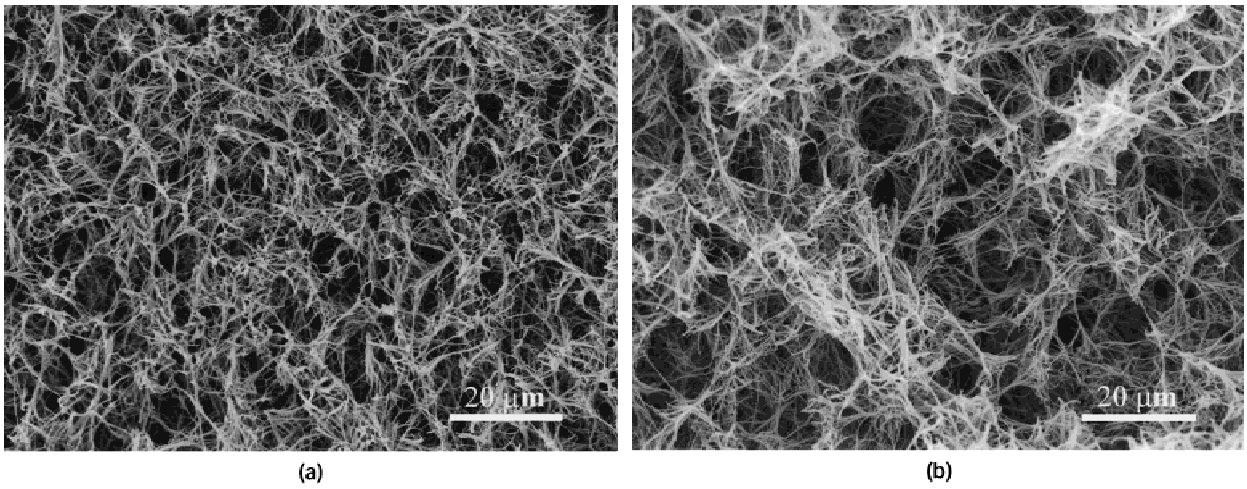

Figure 11. SEM micrographs of PLLA matrices prepared from 5.0% (wt/v) PLLA/THF solution at a gelation temperature of −18°C, and frozen at different temperatures before freeze-drying: (a) liquid nitrogen for 5 min, ×1.0K; (b) −5°C for 5 h, ×1.0K.

room temperature was plateletlike (aggregates of many single crystals) appears to support this hypothesis. For all the studied solvents or solvent mixtures in which PLLA solution can form a gel, both nano-fiber and plateletlike structures have been observed, depending on the gelation temperature. The plateletlike structure forms at a relatively higher gelation temperature, while the nano-fiber structure forms at a lower gelation temperature. To obtain a uniform nanofiber network, the cooling rate must be high enough to avoid polymer crystal nucleation and growth. In some cases such as a PLLA/THF/methanol (80/20) system, the nano-fiber structure can be obtained only by quenching in liquid nitrogen (Fig. 3). We hypothesize that the nano-fibrous structure is formed by spinodal liquid–liquid phase separation of the polymer solutions and consequential crystallization of the polymer-rich phase. This is the first report on the nano-fibrous matrices of aliphatic polyesters. More detailed studies are needed to understand thoroughly the mechanisms of the formation of the nano-fibrous matrices.

It was also found that the final matrix architecture is dependent on thermal history. When a fibrous matrix is formed from a 5% PLLA/THF solution after gelling at −18°C for 10 min (gelation time, 8 min), the morphology [Fig. 8(d)] is not affected by annealing the gel at room temperature (a temperature for platelike structure formation) for 1 week. It is also true that if a plateletlike matrix is formed at room temperature first, the morphology does not change by annealing at −18°C (a temperature for fibrous matrix formation) [Fig. 8(c)]. However, when this polymer solution is first kept at room temperature for a shorter time (e.g., 2 or 12 h) and then cooled down to −18°C, a matrix composed of both small platelets and nano-fibers is formed [Fig 8(a,b)]. The plateletlike structure increases with the annealing time at room temperature. These results suggest that the structure of the PLLA matrix is determined by the initial phase-separated structure.

In the process of water extraction, the translucent or cloudy gel slowly become opaque (white) and strong. Water may have accelerated the coagulation of the PLLA molecular chains, which are still in swelling medium of THF. Water is a nonsolvent for PLLA. When water molecules diffuse into the gel and coexist with THF molecules, the solvating property is changed, and the polymer chains in polymer-rich phase are in a poorer solvent environment. Under this condition, the polymer chains might aggregate rapidly to form a crystal or amorphous solid and rigidify the gel. The small shrinkage of gels (<5%) in the water extraction process may be the result of the polymer chain coagulation. However, the water extraction process has not shown effects on the overall matrix structure formation.

The unit length (fiber length between two conjunctions) of a fibrous matrix is an approximate measure of the pore size and network density based on a simplified cubic structural model. These data are consistent with the morphologic observations in general trend. However, the actual fibrous matrices are not cubic structure. The structural uniformity and pore size distribution are affected by the polymer concentration, gelation temperature, solvent, and freezing temperature (ice crystal formation) before freeze-drying. These processing variables can be used to control the final pore size and size distribution of the matrices.

The weak mechanical properties of the plateletlike matrices are likely due to the loose connections between the platelets. The nano-fibrillar matrices have considerable mechanical strength, presumably due to the continuous fibrous network. The Young's modulus and tensile strength increased with polymer concentration nearly linearly, likely due to the linear in-

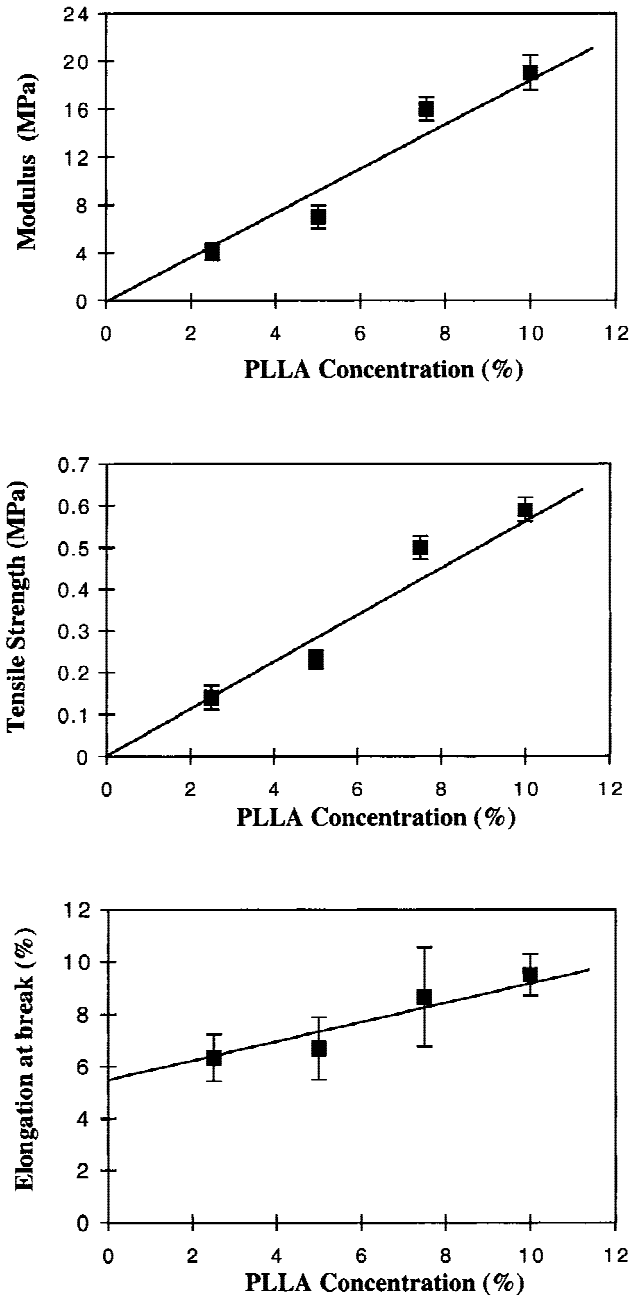

Figure 12. Tensile mechanical properties of fibrous PLLA matrices prepared from PLLA/THF solutions at a gelation temperature of −18°C.

crease in fiber network density. Therefore, the mechanical properties of the nano-fiber matrix can be tailored to specific property needs by adjusting polymer concentration without affecting the fiber diameter with this new fabrication technology.

There are several advantages of the fabrication methods of the fibrous matrices. First, there are almost no equipment requirements compared to the fibrous nonwoven fabric processing with the textile technology.[6] Second, the procedure is greatly simplified, because there is no need to go through many complicated processing stages such as fiber extrusion, drawing, crimping, cutting into stable fibers, carding, needling, heat platen pressing, degreasing, and punching. Third, the diameter of fibers is in the nanometer scale, which is very difficult to achieve, if not impossible, with the textile technology. Fourth, this process can directly fabricate a scaffold into the anatomical shape of a body part with a mold. Fifth, the novel matrix is a continuous fiber network, and may have better mechanical properties compared to mechanically entangled nonwoven structures. Sixth, the average fiber diameter is not affected by the polymer concentration or gelation structure in a large extent, so that the batch-to-batch consistency may be easily achieved.

The surface-to-volume ratio is considered to be a very important structural parameter for polymer scafolds.[7,10] A high surface area is believed to enhance cell attachment. For many cell types, cell migration, growth, and differentiated function are all dependent on cell attachment. The new nano-fibrous matrices have a surface-to-volume ratio (~24 μm^{-1}) much higher than that of either fibrous poly(glycolic acid) nonwoven scaffolds (~0.27 μm^{-1}) fabricated with the textile technology or PLLA foams (~0.03–0.15 μm^{-1}) fabricated with a salt-leaching technique. Therefore, the new synthetic extracellular matrix analogue might provide a better environment for cell attachment, proliferation, and function. A systematic study on the interactions between cells and these nano-fibrous matrices is in progress and will be reported separately.

The authors thank Professor A. F. Yee for generously making his DSC available.

References

1. Langer R, Vacanti J. Tissue engineering. Science 1993;260:920–926.
2. Nerem RM, Sambanis A. Tissue engineering: From biology to biological substitutes. Tissue Eng 1995;1:3–13.
3. Yannas IV. Tissue regeneration by use of collagen-glycosaminoglycan copolymers. Clin Mater 1992;9:179.
4. Natsume T, Ike O, Okada T, Takimoto N, Shimizu Y, Ikada Y. Porous collagen sponge for esophageal replacement. J Biomed Mater Res 1993;27:867–875.
5. Bell E, Rosenberg M, Kemp P, Gay R, Green G, Muthukumaran N, Nolte C. Recipes for reconstituting skin. J Biomech Eng 1991;113:113–119.
6. Ma PX, Langer R. Degradation, structure and properties of fibrous nonwoven poly(glycolic acid) scaffolds for tissue engineering, In: Mikos AG, et al., editors. Polymers in medicine and pharmacy. MRS, Pittsburgh: 1995. p 99–104.
7. Mikos AG, Thorsen AJ, Czerwonka LA, Bao Y, Langer R, Winslow DN, Vacanti JP. Preparation and characterization of poly(l-lactic acid) foams. Polymer 1994;5:1068–1077.
8. Vacanti C, Vacanti J. Bone and cartilage reconstruction with tissue engineering approaches. Otolaryngol Clin North Am 1994;27:263–276.

9. Ma PX, Schloo BS, Mooney D, Langer R. Development of biomechanical properties and morphogenesis of *in vitro* tissue engineered cartilage. J Biomed Mater Res 1995;29:1587–1595.
10. Ma PX, Langer R. Fabrication of biodegradable polymer foams for cell transplantation and tissue engineering. In: Yarmush M, Morgan J, editors. Tissue engineering methods and protocols. Totowa, NJ: Humana Press, 1998. p 47–56.
11. Shinoka T, Ma PX, Shum-Tim D, Breuer CK, Cusick RA, Zund G, Langer R, Vacanti JP, Mayer JE Jr. Tissue-engineered heart valves: Autologous valve leaflet replacement study in a lamb model. Circulation 1996;94(Suppl):II-164–II-168.
12. Elsdale T, Bard J. Collagen substrata for studies on cell behavior. J Cell Biol 1972;54:626–637.
13. Strom SC, Michalopoulos G. Collagen as a substrate for cell growth and differentiation. Methods Enzymol 1982;82:544–555.
14. Grinnell F, Bennett MH. Ultrastructural studies of cell–collagen interactions. Methods Enzymol 1982;82:535–544.
15. Hay ED. Cell biology of extracellular matrix. 2nd edition, New York: Plenum Press; 1991.
16. Cima L, Vacanti J, Vacanti C, Ingber D, Mooney D, Langer R. Tissue engineering by cell transplantation using degradable polymer substrates. J Biomech Eng 1991;113:143–151.
17. Matlaga B, Salthouse T. Ultrastructural observations of cells at the interface of a biodegradable polymer: Polyglactin 910. J Biomed Mater Res 1983;17:185–197.
18. Craig P, Williams J, Davis K, Magoun A, Levy A, Bogdansky S, Jones JJ. A biologic comparison of polyglactin 910 and polyglycolic acid synthetic absorbable sutures. Surg Gynecol Obstet 1975;141:1–10.
19. Cusick RA, Lee H, Sano K, Pollok JM, Utsunomiya H, Ma PX, Langer R, Vacanti JP. The effect of donor and recipient age on engraftment of tissue-engineered liver. J Pediatr Surg 1997;32:357–360.
20. Kim TH, Lee HM, Utsonomiya H, Ma P, Langer R, Schmidt EV, Vacanti JP. Enhanced survival of transgenic hepatocytes expressing hepatocyte growth factor in hepatocyte tissue engineering. Transplant Proc 1997;29:858–860.
21. Ishaug SL, Crane GM, Miller MJ, Yasko AW, Yaszemski MJ, Mikos AG. Bone formation by three-dimensional stromal osteoblast culture in biodegradable polymer scaffolds. J Biomed Mater Res 1997;36:17–28.
22. Ma PX, Shin'oka T, Zhou T, Shum-Tim D, Lien J, Vacanti JP, Mayer J, Langer R. Biodegradable woven/nonwoven composite scaffolds for pulmonary artery engineering in an juvenile lamb model. Trans Soc Biomater 1997;20:295.
23. Vacanti C, Langer R, Schloo B, Vacanti J. Synthetic polymers seeded with chondrocytes provide a template for new cartilage formation. Plast Reconstr Surg 1991;88:753–759.
24. Cao Y, Vacanti J, Ma X, Paige K, Upton J, Chowanski Z, Schloo B, Langer R, Vacanti C. Generation of neo-tendon using synthetic polymers seeded with tenocytes. Transplant Proc 1994;26:3390–3392.
25. Cao Y, Vacanti JP, Ma PX, Paige KT, Upton J, Chowanski Z, Schloo B, Langer R, Vacanti CA. Tissue engineering of neotendon from poly(glycolic acid) scaffolds and tenocytes. In: Mikos AG, Leong KW, Yaszemski MJ, Tamada JA, Radomsky ML, editors. Polymers in medicine and pharmacy. Pittsburgh: MRS, 1995. p 83–89.
26. Vacanti C, Kim W, Upton J, Vacanti M, Mooney D, Schloo B, Vacanti J. Tissue-engineered growth of bone and cartilage. Transplant Proc 1993;25:1019–1021.
27. Shinoka T, Shum-Tim D, Ma PX, Tanel RE, Langer R, Vacanti JP, Mayer JE Jr. Tissue-engineered heart valve leaflets: Does cell origin affect outcome? Circulation 1997;96(Suppl):II-102–II-107.
28. Zund G, Breuer CK, Shinoka T, Ma PX, Langer R, Mayer JE, Vacanti JP. The in vitro construction of a tissue engineered bioprosthetic heart valve. Eur J Cardiothorac Surg 1997;11:493–497.
29. Breuer CK, Shin'oka T, Tanel RE, Zund G, Mooney DJ, Ma PX, Miura T, Colan S, Langer R, Mayer JE, Vacanti JP. Tissue engineering lamb heart valve leaflets. Biotechnol Bioeng 1996;50:562–567.
30. Shinoka T, Breuer CK, Tanel RE, Zund G, Miura T, Ma PX, Langer R, Vacanti JP, Mayer JE Jr. Tissue engineering heart valves: Valve leaflet replacement study in a lamb model. Ann Thorac Surg 1995;60(Suppl):5513–5516.
31. Shinoka T, Shum-Tim D, Ma PX, Tanel RE, Isogai N, Langer R, Vacanti JP, Mayer JE Jr. Creation of viable pulmonary artery autografts through tissue engineering. J Thorac Cardiovasc Surg 1998;115:536–545.
32. Jamshidi K, Hyon SH, Ikada Y. Thermal characterization of polylactides. Polymer 1988;29:2229–2234.
33. Fischer EW, Sterzel HJ, Wegner G. Investigation of the structure of solution grown crystals of lactide copolymers by means of chemical reactions. Kolloid-Zeitschrift Zeitschrift Polymere 1973;251:980–990.
34. Coombes AG, Heckman JD. Gel casting of resorbable polymers: 2. In-vitro degradation of bone graft substitutes. Biomaterials 1992;13:297–307.
35. Agrawal CM, Best J, Heckman JD, Boyan BD. Protein release kinetics of a biodegradable implant for fracture non-unions. Biomaterials 1995;16:1255–1260.
36. Hubbell JA, Massia SP, Drumheller PD. Surface-grafted cell-binding peptides in tissue engineering of the vascular graft. Ann NY Acad Sci 1992;665:253–258.
37. Lin HB, Sun W, Mosher DF, Garcia-Echeverria C, Schaufelberger K, Lelkes PI, Cooper SL. Synthesis, surface, and cell-adhesion properties of polyurethanes containing covalently grafted RGD-peptides. J Biomed Mater Res 1994;28:329–342.
38. Dee KC, Rueger DC, Andersen TT, Bizios R. Conditions which promote mineralization at the bone–implant interface: A model in vitro study. Biomaterials 1996;17:209–215.
39. Rezania A, Thomas CH, Branger AB, Waters CM, Healy KE. The detachment strength and morphology of bone cells contacting materials modified with a peptide sequence found within bone sialoprotein. J Biomed Mater Res 1997;37:9–19.
40. Zhang R, Ma PX. Poly(alpha-hydroxy acids)/hydroxyapatite porous composites for bone tissue engineeering: 1. Preparation and morphology. J Biomed Mater Res 1999;44:446–455.
41. Zhang R, Ma PX. Porous poly(L-lactic acid)/apatite composites created by a biomimetic process. J Biomed Mater Res 1999;45:285–293.
42. Hollinger JO, Schmitz JP. Macrophysiologic roles of a delivery system for vulnerary factors needed for bone regeneration. Ann NY Acad Sci 1997;831:427–437.
43. Hollinger JO, Leong K. Poly(alpha-hydroxy acids): Carriers for bone morphogenetic proteins. Biomaterials 1996;17:187–194.
44. Schugens C, Grandfils C, Jerome R, Teyssie P, Delree P, Martin D, Malgrange B, Moonen G. Preparation of a macroporous biodegradable polylactide implant for neuronal transplantation. J Biomed Mater Res 1995;29:1349–1362.
45. Hsu YY, Gresser JD, Stewart RR, Trantolo DJ, Lyons CM, Simons GA, Gangadharam PR, Wise DL. Mechanisms of isoniazid release from poly(d,l-lactide-co-glycolide) matrices prepared by dry-mixing and low density polymeric foam methods. J Pharmaceut Sci 1996;85:706–713.
46. Lo H, Kadiyala S, Guggino SE, Leong KW. Poly(L-lactic acid) foams with cell seeding and controlled-release capacity. J Biomed Mater Res 1996;30:475–484.
47. Athanasiou KA, Niederauer GG, Agrawal CM. Sterilization, toxicity, biocompatibility and clinical applications of polylactic acid/polyglycolic acid copolymers. Biomaterials 1996;17:93–102.